Effects of Dust Characteristics on Hot-Gas Filter Performance in a Transport Reactor System

R. S. Dahlin and E. C. Landham
Southern Research Institute, P.O. Box 1069, Wilsonville, AL 35186

Abstract

This paper discusses the use of in-situ particulate sampling and ash characterization in analyzing the performance of a hot-gas filter installed on a transport reactor system at the Power Systems Development Facility (PSDF). In-situ measurements of the particulate loadings entering and leaving the hot-gas filter have been made during combustion-mode operation of the transport reactor system with four different fuels (three coals and one petroleum coke) and with four different desulfurization sorbents (one dolomite and three limestones). Inlet particulate loadings have varied from about 6,000 ppmw to 21,000 ppmw. Outlet particulate loadings have been as low as 0.2 ppmw when all filter elements are intact and properly sealed in the tubesheet. When filter elements are broken or seals are compromised, the outlet loading has been as high as 22 ppmw.

Studies of ash dropout in the filter vessel have shown that about 26 to 28% of the ash entering the filter vessel drops out before reaching the filter elements. Drag measurements made on inlet particulate samples that were sieved to simulate the effects of dropout were in good agreement with corresponding values of transient filter drag based on the filter ΔP, face velocity, and areal dustcake loading. Drag measurements made on residual dustcake samples were in reasonably good agreement with the baseline ΔP, after the baseline ΔP was adjusted for pressure losses across the filter elements themselves and in other portions of the vessel.

Studies of dustcake layers suggest that there are significant differences between the residual and transient dustcakes in terms of chemical composition, particle-size distribution, porosity, and drag. Results obtained to date suggest that the transient dustcake is more porous than the residual dustcake and offers less resistance to gas flow than does the residual dustcake. These differences should be taken into account in the analysis and modeling of hot-gas filter performance.

Keywords: filtration, filtration performance, filtration properties, dust, dust characterization, filter cake

1. Introduction

Successful commercialization of advanced coal-based power generation technologies will require highly efficient removal of ash particles from gas streams at elevated temperatures and pressures. Particulate loadings must be maintained at very low levels (e.g., <20 ppmw), and the concentration of large (>5-μm) particles must be minimized to ensure the reliable operation of downstream combustion turbines in these environments. Previous studies have suggested that ceramic and metallic candle filters can be used to meet these ambitious goals, but problems remain with the reliability of filter elements, failsafes, and sealing systems (Dennis, 1998). At elevated operating temperatures above about 820°C (1500°F), some test facilities have also reported filter element failures caused by ash bridging (Mudd and Hoffman, 1995; Seville, 1996). At the Power Systems Development Facility (PSDF), filter operating temperatures have been limited to about 760°C (1400°F), and there have been no serious problems with ash bridging during coal combustion. However, there has recently been one incident of ash bridging in the hot-gas filter after about 30 hours of operation on petroleum coke and dolomite. Since petroleum coke is much less expensive than coal, there is a strong economic incentive to solve this ash bridging problem. The cause of the ash bridging is under investigation, but no conclusions have yet been reached. Other recent work at the PSDF has highlighted the need for more reliable filter elements, failsafes, and sealing systems (Scarborough *et al*, 1999; Davidson *et al*, 1999).

In building the next generation of coal-fired power plants, utilities will require a conservatively sized hot-gas filter system. The design of the system must ensure that the filter pressure drop will be maintained within acceptable limits, in terms of both the baseline and peak values. To satisfy this requirement, the designer will need dependable data on the drag, or flow resistance, exerted by the residual dustcake, as well as the drag exerted by the transient dustcake that is built up during each filtration cycle. To provide this information, the filter test program at the PSDF includes sampling and characterization of ash entering the hot-gas filter and residual and transient dustcakes collected during various tests. At the PSDF, it is the goal of the particulate sampling and characterization program to provide the data needed to understand hot-gas filter performance and to design hot-gas filters for future commercial applications.

2. In-Situ Particulate Sampling Systems

The in-situ particulate sampling systems currently in use at the PSDF (Figure 1) have been described in detail elsewhere (Dahlin *et al*, 1998). These systems make it possible to isokinetically collect particulate samples directly from the

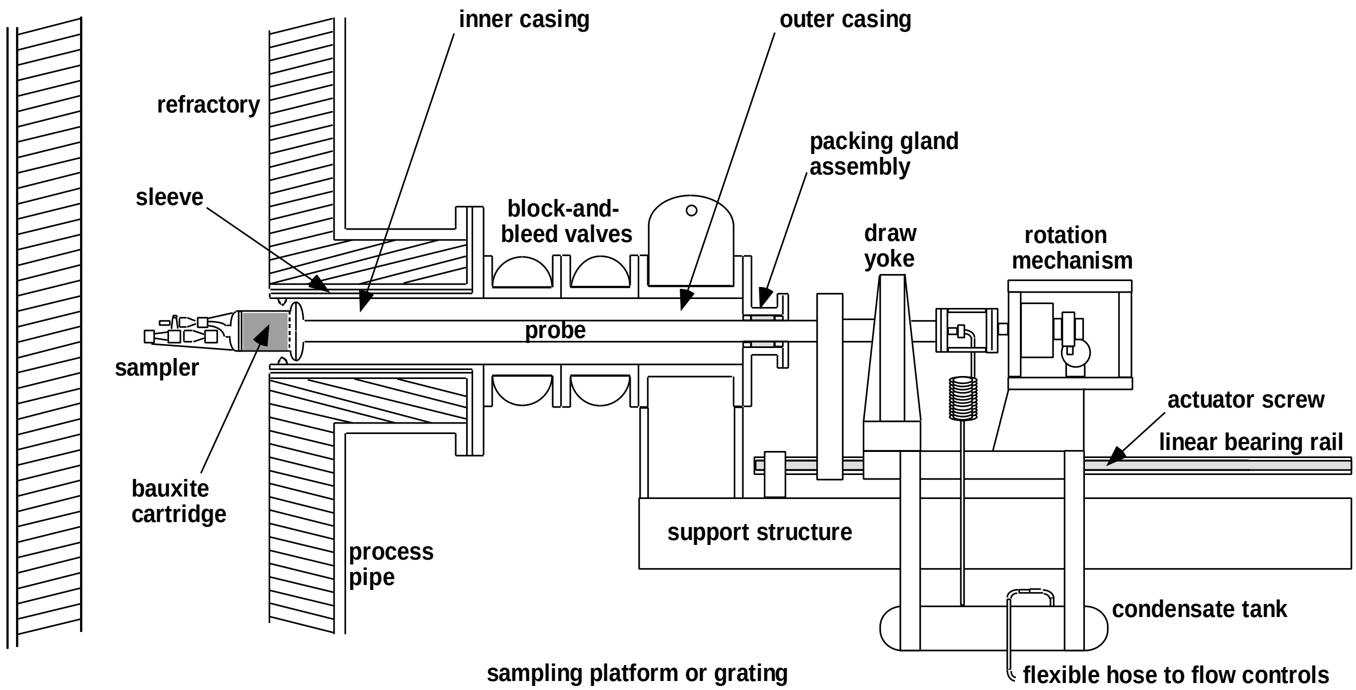

Figure 1. Simplified Drawing of In-Situ Particulate Sampling System

process gas streams entering and leaving the hot-gas filter. The samples are collected in situ at process temperature and pressure, thereby minimizing any loss or alteration of particles in the sampling system. This approach represents a significant improvement over the extractive sampling systems that have been used elsewhere. Particles passed through extractive sampling lines undergo numerous collisions with the walls of the sampling lines and can be reentrained as larger agglomerates, thus altering their particle-size distribution (Anand *et al*, 1992). Heat loss and condensation can cause further alteration of particle properties as the particles are transported through extractive sampling lines. At the PSDF, these problems are avoided by the use of *in-situ* sampling.

3. Particulate Loadings and Filter Collection Efficiency

Table 1 gives a summary of the particulate loadings measured in the flue gas stream entering the hot-gas filter. As indicated in the table, the measured loadings have typically varied from about 6,000 to 15,000 ppmw and generally follow the expected trend based on fuel ash content, fuel sulfur content, and sorbent addition rate. Much higher inlet loadings have been measured on a few occasions, but these excursions were traced to upsets in the solids recirculation system, which caused a temporary carryover of bed material.

Table 2 gives a summary of the particulate collection performance of the hot-gas filter during each of the major test segments. As indicated in the table, these results show that the hot-gas filter system is capable of achieving outlet particle loadings of about 0.2 ppmw when there are no sealing problems and all of the elements are intact. An average outlet loading of 0.2 ppmw was measured at the beginning of the first major test segment even though one filter element was broken. Later in the test, a second element was broken, and the average outlet loading increased to about 7 ppmw. These results suggest that the first failsafe operated as intended, but the second one failed to plug completely. Thus, the failsafes currently in use at the PSDF have not provided consistent protection against filter element failures.

With broken elements or sealing problems, outlet loadings as high as 13 ppmw have been measured at a filter face velocity of 2.5 to 3 cm/sec (5 to 6 ft/min). At a filter face velocity of 4 cm/sec (8 ft/min.), particle penetration has been as high as 22 ppmw with leakage between the element/failsafe assembly and the tubesheet. In one instance there was a massive leak through a failsafe that had been modified by insertion of a thermocouple feedthrough: the outlet particle loading was 720 ppmw in this case. Although this type of feedthrough would never be installed in a commercial system, this high level of emissions indicates how high the outlet loading could become without failsafes and clearly demonstrates the need for reliable failsafes.

4. Particle Dropout in Filter Vessel

Particulate samples collected from the gas stream entering the filter vessel may not accurately reflect the characteristics of the particles arriving at the filter elements, because larger particles inertially separate from the flue gas in the filter

Table 1. Comparison of Average Particulate Loadings Measured in Situ and Calculated Based on 100% Carryover of Coal Ash and Sorbent Reaction Products

Coal	Ash, Wt %	Sulfur, Wt %	Sorbent	Wt Ratio, lb/lb (Ash+Reacted Sorbent)/Coal[1]	Calculated Loading, ppmw[2]	No. of In-Situ Samples	In-Situ Average, ppmw	In-Situ Std Dev, ppmw	Apparent Carryover, %
Alabama	15-16	0.8-1.0	Dolomite	0.24	12,000	20	11,500	2,300	96
Alabama	15-16	0.8-1.0	Ohio LS	0.21	10,500	2	9,900	2,900	94
Alabama	15-16	0.8-1.0	Alabama LS	0.21	10,500	3	9,900	1,500	94
Eastern Kentucky	8-9	1.3-1.4	Dolomite	0.20	10,000	2	8,800	600	88
Eastern Kentucky	8-9	1.3-1.4	Ohio LS	0.17	8,500	3	7,400	1,100	87
Eastern Kentucky	8-9	1.3-1.4	Alabama LS	0.17	8,500	3	6,400	1,100	75
Eastern Kentucky	8-9	1.3-1.4	Gregg LS	0.17	8,500	4	6,200	700	73
Illinois	7-11	3.5	Ohio LS	0.30	15,000	4	14,800	1,000	99
Illinois	7-11	3.5	Alabama LS	0.30	15,000	2	14,600	1,600	97
Petroleum Coke	0.5	5	Dolomite	0.43	21,500	5	21,100	4,200	98
Petroleum Coke	0.5	5	Ohio LS	0.30	15,000	2	14,100	2,800	94

1. Calculated based on Ca/S molar ratio of 2:1 and calcium utilization of 50%.
2. Calculated based on 20 lb of flue gas per lb of coal.

Table 2. Summary of Hot-Gas Filter Particulate Collection Performance During Major Test Segments

Dates	Average Inlet Loading, ppmw	Average Outlet Loading, ppmw	Average Efficiency, %	Notes
Beginning of TC01. Filter element fragments found in ash discharge system during startup.				
9/9/97 to 9/19/97	**11,400**	**0.22**	**99.998**	**One broken element.**
Additional filter element fragments found in ash discharge system. Continuation of TC01.				
9/25/97 to 10/30/97	**11,500**	**7.2**	**99.94**	**Two broken elements.**
Thermal excursion. All Coors elements broken. System shut down and Coors elements replaced with 3M elements.				
12/1/97 to 12/8/97	**10,900**	**4.3**	**99.96**	**No broken elements. Suspect sealing problem.**
Beginning of TC02. Filter element fragments found in ash discharge system during startup.				
4/13/98	**11,400**	**720**	**93.7**	**Massive leak through thermocouple feedthrough.**
Seven broken elements replaced. Thermocouple feedthrough in failsafe eliminated. Continuation of TC02.				
4/23/98 to 5/13/98	**10,200**	**7.1**	**99.93**	**Suspect sealing problem with 3M elements.**
Inserts installed in 3M elements to improve sealing. Smooth startup for TC03.				
6/5/98 to 8/10/98	**8,900**	**0.21**	**99.998**	**Over 800 hrs with no leakage.**
Removed filter elements to operate at higher face velocity (8 ft/min.).				
1/18/99 to 1/22/99	**10,100**	**15.8**	**99.84**	**Suspect sealing problems at higher** D**P.**
Full compliment of elements installed to restore original face velocity (5 to 6 ft/min.).				
2/3/99 to 2/19/99	**13,500**	**4.6**	**99.97**	**Sealing problems reduced but not eliminated.**

vessel. In filter vessels that have a tangential entrance—like the one on the transport reactor system—swirling gas flow probably enhances this separation of larger particles. Patterns of ash deposition on the filter vessel shroud and on the outer circle of filter elements suggest that the swirl persists as the gas flows over and under the shroud and reaches the filter elements. Because of this effect, the dustcakes on the outer circle of filter elements typically have a well-defined ridge on the windward side where the gas flow impacts against the elements.

To estimate the magnitude of the ash dropout, a series of tests were done in which the ash that dropped out between backpulses was collected separately from the ash that was pulsed off the filter elements. Thermocouples in the ash discharge system were used to track the ash movement through the discharge system and to distinguish between dropout ash and backpulsed ash. The dropout ash and backpulsed ash were collected separately in preweighed drums to determine the weight fraction of ash that dropped out in the vessel. Based on these tests, it was estimated that 26 to 28 wt% of the incoming ash dropped out before reaching the elements. The actual percentage of dropout will vary with changes in the incoming particle-size distribution and in the gas velocity between the shroud and the outer circle of elements. As total gas flow is increased, the incoming size distribution will become finer as a result of more efficient particle separation in the primary cyclone. The reduction in particle size will result in reduced particle dropout in the filter vessel. At the same time, the higher gas velocity between the shroud and elements may tend to enhance particle removal.

To assess the impact of particle dropout on the particle-size distribution and other characteristics of the dustcake, particle-size analyses were done on samples of dropout ash and samples of backpulsed ash. The particle-size distributions were used to calculate the particle dropout—or removal—efficiency as a function of particle size. The resulting removal efficiency curve (see Figure 2) clearly illustrates that the dropout is a strong function of particle size. Almost all of the particles larger than 100 μm drop out; while there is relatively little removal of particles smaller than about 45 μm. The fine-particle portion of the removal efficiency curve is probably a reflection of agglomerates that dropped out in the filter vessel and were then broken into smaller particles during the particle-size analysis.

Because of particle dropout in the filter vessel, it is to be expected that the particle-size distribution of the transient dustcake collected during each filtration cycle will be somewhat finer than the particle-size distribution of the ash entering the filter vessel. Particle-size analyses have confirmed this difference. In-situ particulate samples collected at the filter inlet typically have mass-median diameters (mmd's) in the range of 15 to 20 μm. Transient dustcake samples taken after a dirty shutdown of the hot-gas filter typically have mmd's in the range of 9 to 14 μm.

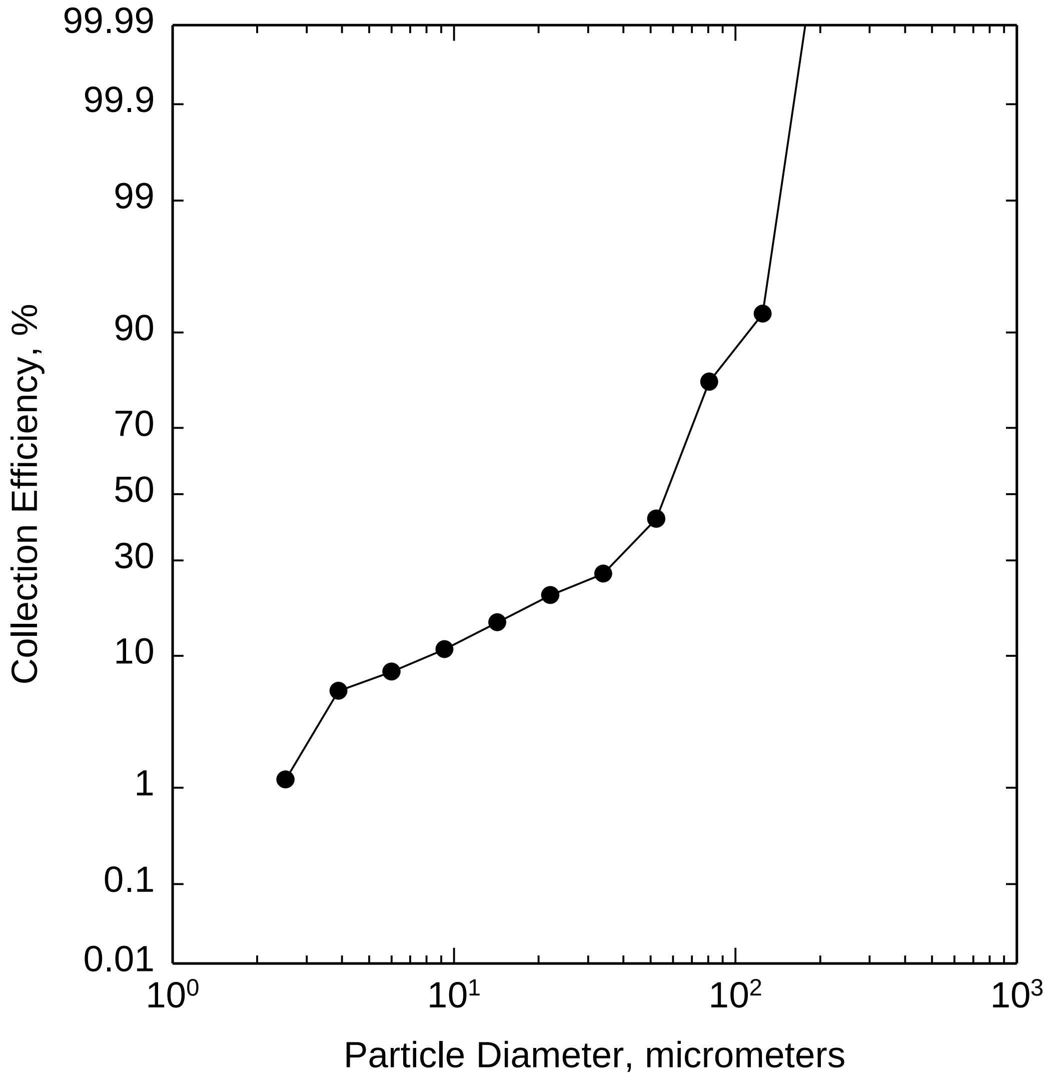

Figure 2. Ash Dropout Efficiency as a Function of Particle Size

5. Characterization of Residual and Transient Dustcakes

At any point in a filtration cycle, the pressure drop across a filter system is influenced by the drag of the dustcake, which is a function of the dustcake particle-size distribution, porosity, and thickness (or areal loading). To study the effects of these parameters on hot-gas filter performance, dustcake samples have been collected during each inspection of the filter internals. During early tests of the hot-gas filter system, the filter was typically pulse-cleaned during shutdown and prior to inspection. The dustcake samples removed after these shutdowns represent the residual dustcake that remains on the filter elements after pulse cleaning. The characteristics of these residual dustcake samples are important in understanding changes in the baseline pressure drop across the filter. Residual dustcake samples collected at the PSDF have typically had mmd's of 8 to 9 µm. The thicknesses of the residual dustcakes have typically been in the range of 3 to 5 mm (1/8 to 3/16 in.). Based on a single set of measurements, the areal loading of the residual dustcake was determined to be 0.2 to 0.24 g/cm^2 (0.4 to 0.5 lb/ft^2), and the porosity of the residual dustcake was determined to be 74 to 79%. Because of the limited data on these parameters, these values of areal loading and porosity may not necessarily be typical of the residual dustcake.

In analyzing the additional pressure drop that builds up during the filtration cycle, it is important to understand the properties of the transient dustcake that is accumulated and removed with each filtration and cleaning cycle. To allow sampling of the transient dustcake (as well as the residual dustcake), the hot-gas filter system has sometimes been shut down in a dirty condition. In one of these dirty shutdowns, the transport reactor system is shut down near the end of a filtration cycle without any subsequent pulse cleaning of the filter. The gas flow through the filter is reduced as quickly as possible to minimize any additional compression of the dustcake and to preserve the entire (residual-plus-transient) dustcake on the filter elements. Special sampling techniques, which are discussed below, are then used to obtain separate samples of the outer layer and inner layer of the dustcake.

In general, residual dustcakes are exposed to the hot flue gas for time periods that are much longer than the exposure times of transient dustcakes. Since sorbent sulfation is still proceeding at a significant rate at 760°C (1400°F), the residual dustcake gradually becomes more highly sulfated than the transient dustcake. Since calcium sulfate has a larger molar volume than does calcium oxide, the structure of the dustcake must change as the sulfation reaction proceeds. Long-term changes in dustcake structure may also be brought about by consolidation of individual particles through the formation of low-melting eutectic mixtures (Snyder and Pontius, 1998). Over time, the sulfation and consolidation reactions could produce a gradual increase in particle size and a gradual decrease in porosity of the residual dustcake. Other mechanisms that could affect the residual dustcake particle size and porosity include preferential penetration of smaller particles into the residual dustcake and preferential removal of larger particles during pulse cleaning. Over time, these mechanisms could produce a gradual decrease in particle size and a gradual increase in porosity.

To investigate the differences between residual and transient dustcakes, a special sampling procedure was developed to collect separate samples of the inner and outer layers of a dustcake. The procedure uses a contoured scraper that is designed to remove an outer layer of the dustcake, leaving behind a layer that is about 5-mm (3/16-in.) thick. This thickness was chosen to correspond roughly with previous measurements of the residual dustcake thickness. Although this separation of the dustcake layers may not correspond precisely to the location of the boundary between the residual and transient dustcakes, this type of sampling should be sufficient to reveal any differences between these layers.

The layered sampling procedure was first used after a dirty shutdown performed in May 1998. Three sets of residual and transient dustcake samples were collected and characterized. In terms of particle size, drag, and chemistry, the results showed consistent differences between the residual and transient dustcake samples (see table on next page). As shown in the tabulated results, the residual dustcakes were more fully sulfated and had smaller mean particle sizes, lower porosities, and more resistance to gas flow (higher drag).

The dustcake drag reported here was interpolated from a series of drag measurements made in a laboratory test cell at room temperature over a range of dustcake porosities. The drag values are applicable to the corresponding porosity values given in the table. The porosities are estimated values determined from measurements of the areal loading and thickness made on the entire (residual-plus-transient) cake and measurements of areal loading and thickness of residual dustcakes from previous tests. The difference in residual and transient dustcake porosity (76% versus 82%) is significant and is a major determining factor in the higher flow resistance of the residual cake. Comparisons of laboratory drag measurements with actual baseline and peak ΔP values confirm that these differences are real and are in fact necessary to explain the observed trends in filter ΔP.

	Residual Dustcake	Transient Dustcake
Sulfate content, wt%	19.1 ± 2.9	9.5 ± 0.4
Sorbent utilization (Ca+Mg), %	100	37 ± 6
Mass-median diameter, μm	9.0 ± 0.5	11.4 ± 2.5
Porosity, %	76 ± 1	82 ± 1
Drag, mbar/(cm/sec)/(g/cm^2)	153 ± 10	46 ± 5
Drag, in H_2O/(ft/min)/(lb/ft^2)	15 ± 1	4.5 ± 0.5
Drag-equivalent diameter, μm	1.8 ± 0.1	2.1 ± 0.1

From these results, it is clear that these residual and transient dustcake samples are characterized by substantial differences in their resistance to gas flow. These differences must be taken into account when analyzing the performance of the hot-gas filter. The baseline pressure drop across the filter just after cleaning will be governed by the properties of the residual dustcake. The properties of the transient dustcake will govern the additional pressure drop that is accumulated during the filtration cycle.

6. Residual Dustcake Characteristics and Baseline Pressure Drop

The baseline pressure drop across a hot-gas filter system just after cleaning may be separated into three components: (1) the pressure drop across the residual dustcake, (2) the pressure drop across the filter element itself, and (3) other pressure losses associated with flow in the vessel internals. The pressure drop attributable to the filter elements and vessel internals may be inferred from the observed ΔP during a system startup on propane in the absence of solids carryover to the filter (i.e., when there is no dustcake on the elements). The clean system ΔP recorded during the startup for the first test segment was about 45 mbar (18 in. H_2O) when corrected to the same face velocity and gas viscosity achieved during stable operation on coal and dolomite with the filter at 760°C (1400°F). With the same array of filter elements in place, the stable baseline ΔP during the first test segment with coal and dolomite was about 175 mbar (70 in. H_2O) at a filter face velocity of 2.3 cm/sec (4.6 ft/min.). Thus, the ΔP across the residual dustcake during this test segment was 130 mbar (52 in. H_2O).

Measurements made on the residual dustcake at the conclusion of this test segment indicated that the average dustcake areal loading was 0.23 g/cm^2 (0.47 lb/ft^2). Thus, the normalized drag exerted by the residual dustcake may be calculated as follows:

Drag = 52 in. H_2O / (4.6 ft/min) / (0.47 lb/ft^2) = 24 in. H_2O/(ft/min)/(lb/ft^2)
= 130 mbar / (2.3 cm/sec) / (0.23 g/cm^2) = 246 mbar/(cm/sec)/(g/cm^2)

The normalized dustcake drag measured in the laboratory at a porosity of 76% and at room temperature was 110 mbar/(cm/sec)/(g/cm^2) or 11 in. H_2O/(ft/min)/(lb/ft^2). To calculate the corresponding drag on the residual cake during operation, this laboratory value of normalized drag has to be corrected to filter conditions by multiplying by the ratio of the flue gas viscosity at process conditions (≈400 μP) to the viscosity of air at room temperature (≈180 μP).

Drag = 110 mbar/(cm/sec)/(g/cm^2) • (400 μP) / (180 μP)
= 244 mbar/(cm/sec)/(g/cm^2)
or

Drag = 11 in. H_2O/(ft/min)/(lb/ft^2) • (400 μP) / (180 μP)
= 24 in. H_2O/(ft/min)/(lb/ft^2)

The calculations shown above illustrate that the laboratory drag measurements are consistent with the observed baseline ΔP of the filter. Conversely, if representative dust samples can be obtained, these results suggest that the corrected laboratory drag measurements can be used in sizing a new filter to meet a specified baseline ΔP.

7. Transient Dustcake Characteristics and Peak Pressure Drop

An analysis similar to the one discussed above can be used to rationalize the available information on transient dustcake drag and peak pressure drop. In the transient analysis, the actual drag of the transient dustcake is determined from the buildup of ΔP during a selected portion of the filtration cycle. The corresponding areal loading of dust is calculated from the particulate loading measured during the selected time interval, the average gas flow during the time interval, and the fraction of ash that drops out in the filter vessel. The ash dropout is taken into account by applying the dropout efficiency curve (Figure 2) to the particle-size distribution of the particulate sample collected during the corresponding time interval.

Figure 3 shows a comparison between transient dustcake drag values calculated by the above procedure and drag measurements made in the laboratory using in-situ particulate samples that were collected during the same time period. The in-situ particulate samples were sieved to account for particle dropout in the filter vessel. The laboratory drag values were obtained using a dustcake porosity equal to the uncompacted bulk porosity of each sample. The values of uncompacted bulk porosity ranged from 80 to 83% for these particular samples. (Recall that the transient dustcake porosity was estimated to be 82% based on previous measurements of dustcake areal loading and thickness.) After correcting the laboratory drag data to 760°C (1400°F) by taking into account the effect of gas viscosity, the laboratory drag measurements closely track the actual drag determined from filter ΔP. This result confirms that the true porosity of the transient dustcake must be close to the estimated value of 82%. In any case, the porosity of the transient dustcake must be significantly higher than that of the residual dustcake in order to explain the observed buildup of pressure drop during the filtration cycle.

While the corrected lab measurements closely track the transient ΔP of the filter, the lab measurements seem to be systematically biased toward somewhat higher values of drag. Such a systematic bias could result from the use of measured values of uncompacted bulk porosity that are lower than the actual porosity of the transient dustcake. Another factor that could bias the results might include a failure of the sieving procedure to accurately simulate the effects of particle dropout.

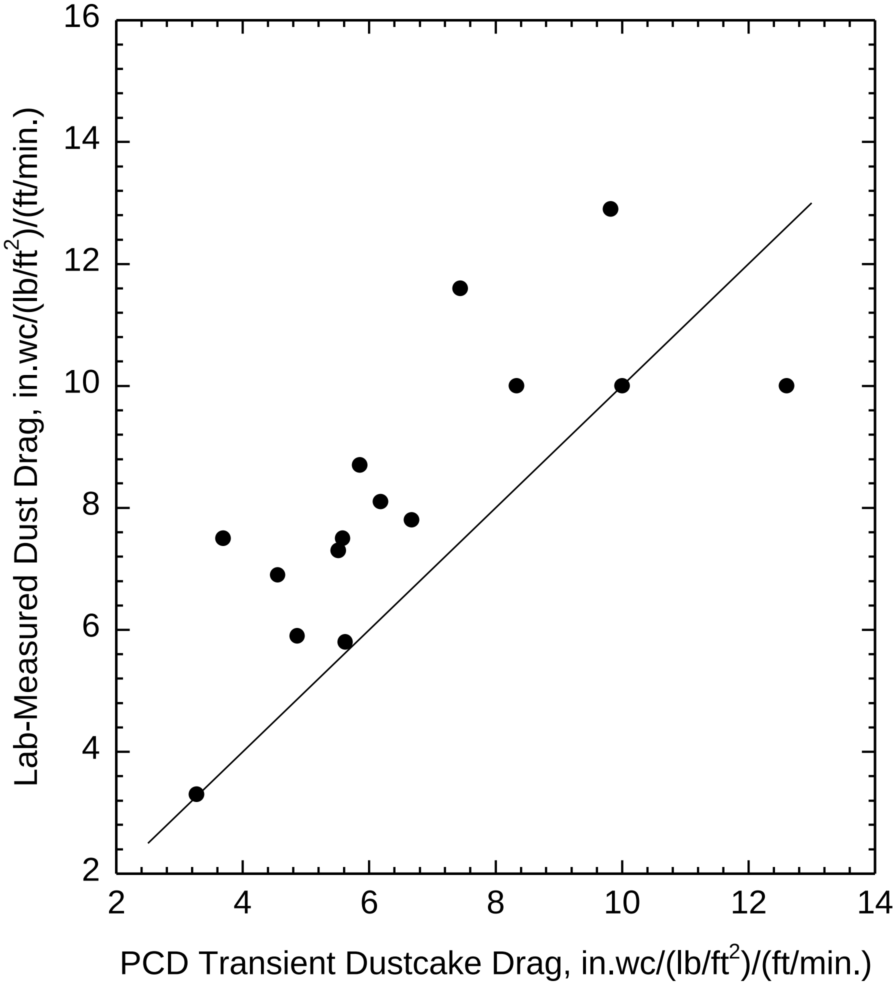

Figure 3. Comparison of Laboratory Drag Measurements Made on In-Situ Particulate Samples with Drag Calculated from Filter Pressure Drop

In the standard drag measurement procedure that has been used to date, the particulate sample is compacted with a piston to produce dustcakes of varying porosity. This type of compaction may not adequately simulate the dustcake compression that takes place as hot flue gas flows through the dustcake. To study the porosity changes produced by flow-induced compression (versus compaction with a piston), a flow-type drag tester has been built. In this apparatus, a particulate sample is suspended in an air stream using an eductor and then collected on a filter at a realistic face velocity. To simulate the dustcake drag at filter conditions, the face velocity used in the testing, V_t, must be higher than the actual filter face velocity, V_f, because of the difference in gas viscosity. Since drag is proportional to gas viscosity,

$$V_t = V_f \bullet \mu_f / \mu_t = V_f \bullet 400\ \mu P / 180\ \mu P = V_f \bullet 2.2$$

Thus, a test velocity of 5.6 cm/sec (11 ft/min.) must be used for room-temperature tests intended to simulate the effects of a filter face velocity of 2.5 cm/sec (5 ft/min.) at 760°C (1400°F).

8. Conclusions

In-situ particulate measurements have demonstrated that the PSDF hot-gas filter is capable of achieving outlet loadings as low as 0.2 ppmw, corresponding to collection efficiencies as high as 99.998%. In actual practice, this level of performance has been achieved in only two of the eight major test segments conducted at the PSDF. With broken filter elements and/or sealing problems, outlet loadings have varied from about 4 to 22 ppmw. Based on the particulate measurements, it is clear that the failsafe devices and sealing system that are currently in use at the PSDF do not provide adequate assurance of acceptable particulate control. Improved failsafe design and sealing system design are needed for successful commercialization of hot-gas filtration technology.

Studies of the PSDF filter dustcakes have shown that there can be significant differences between residual and transient dustcakes, in terms of both chemical composition and physical properties. The residual dustcakes can be more highly sulfated and have smaller mean particle sizes and lower porosities than the transient dustcakes. Preliminary laboratory measurements suggest that these differences can cause the normalized drag of the residual dustcake to be three times higher than the normalized drag of the transient dustcake. Drag measurements made on the residual dustcake appear to be consistent with observed values of baseline ΔP and residual dustcake areal loading. The transient ΔP and areal loading determined from in-situ sampling (corrected for particle dropout) appear to be generally consistent with drag measurements made on in-situ particulate samples that were sieved to account for particle dropout.

Dustcake drag is a very strong function of dustcake porosity, which is frequently unknown or difficult to determine. Uncertainty in dustcake porosity, which has proven to be a major impediment to making meaningful drag measurements, will be reduced through the use of a flow-type drag tester designed to allow the formation of more realistic dustcakes in the laboratory.

9. Acknowledgments

The Power Systems Development Facility is operated under a Cooperative Agreement between the U. S. Department of Energy (DOE) and Southern Company Services (SCS). Kellogg, Brown & Root; Foster Wheeler USA; and Siemens-Westinghouse have provided additional technical and financial support. The work described herein was performed under a subcontract between SCS and Southern Research Institute. The Project Managers responsible for this work are: Mr. James Longanbach (DOE), Mr. Howard Hendrix (SCS), and Dr. Duane Pontius (Southern Research). The authors would also like to acknowledge Southern Research technicians, Mr. Terry Hammond and Mr. Jamie Barrett, who performed the particulate sampling and drag measurements.

10. References

Anand, N. K., A. R. McFarland, K. D. Kihm, and F. S. Wong. *Optimization of Aerosol Penetration Through Transport Lines*. Aerosol Science and Technology, Vol. 16, pp. 105-112 (1992).

Dahlin, R. S., E. C. Landham, and H. L. Hendrix. *In-Situ Particulate Sampling and Characterization at the Power Systems Development Facility*. Aerosol Science and Technology, Vol. 29, pp. 170-182 (1998).

Davidson, M. D., X. Guan, H. L. Hendrix, and P. T. Scarborough. *Power Systems Development Facility: High-Temperature, High-Pressure Filter System Operation in a Combustion Gas*. 4th International Symposium on Gas Cleaning at High Temperatures. Karlsruhe, Germany. September 22-24, 1999.

Dennis, R. A. and M. Epstein (Eds). *Proceedings of the Symposium on High-Temperature Particulate Cleanup for Advanced Coal-Based Power Systems*. Birmingham, Alabama. April 20-23, 1998.

Mudd, M. J. and J. D. Hoffman. *Operating Experience from the Tidd PFBC Hot Gas Cleanup Program*. Proceedings of the 13th International Conference on Fluidized-Bed Combustion. Orlando, Florida. May 7-10, 1995.

Scarborough, P. T., H. L. Hendrix, M. D. Davidson, X. Guan, R. S. Dahlin, and E. C. Landham. *Power Systems Development Facility: High-Temperature, High-Pressure Filter System Operations in a Combustion Gas*. Proceedings of the 44th ASME Gas Turbine and Aeroengine Technical Congress. Indianapolis, Indiana. June 7-10, 1999.

Seville, J. P. K. *Hot-Gas Particulate Cleanup: Current Technological and Commercial Status*. Report No. COAL R092. ETSU. Harwell, U.K. 1996.

Snyder, T. R. and D. H. Pontius. *Characteristics and Behavior of Ash Deposits in Hot Gas Filters*. Proceedings of the Symposium on High-Temperature Particulate Cleanup for Advanced Coal-Based Power Systems. Birmingham, Alabama. April 20-23, 1998.